ELSEVIER

Neurobiology of Disease

www.elsevier.com/locate/ynbdi
Neurobiology of Disease 20 (2005) 574 – 582

Apolipoprotein D is a component of compact but not diffuse amyloid-beta plaques in Alzheimer's disease temporal cortex ☆

Purnima P. Desai,[a,1] Milos D. Ikonomovic,[b,c,1] Eric E. Abrahamson,[b] Ronald L. Hamilton,[d] Barbara A. Isanski,[b] Caroline E. Hope,[b] William E. Klunk,[c] Steven T. DeKosky,[a,b,c] and M. Ilyas Kamboh[a,c,*]

[a]*Department of Human Genetics, Graduate School of Public Health, University of Pittsburgh, Pittsburgh, PA 15261, USA*
[b]*Department of Neurology, University of Pittsburgh School of Medicine, Pittsburgh, PA 15213, USA*
[c]*Department of Psychiatry, University of Pittsburgh School of Medicine, Pittsburgh, PA 15213, USA*
[d]*Department of Neuropathology, University of Pittsburgh School of Medicine, Pittsburgh, PA 15213, USA*

Received 15 December 2004; revised 31 March 2005; accepted 9 April 2005
Available online 23 May 2005

Apolipoprotein D (apoD) is elevated in Alzheimer's disease (AD) cortex, localizing to cells, blood vessels, and neuropil deposits (plaques). The role of apoD in AD pathology and the extent of its co-distribution with diffuse (amorphous) and compact (dense fibrillar) amyloid-beta (Aβ) plaques are currently unclear. To address this issue, we combined apoD and Aβ immunohistochemistry with ThioS/X-34 staining of the β-pleated sheet protein conformation in temporal cortex from 36 AD patients and 12 non-demented controls. ApoD-immunoreactive, Aβ-immunoreactive, and ThioS/X-34-stained plaques were detected exclusively in AD tissue. Dual-immunolabeling showed that 63% of Aβ plaques co-localized apoD. All apoD plaques contained Aβ protein and ThioS/X-34 fluorescence. Compared to controls, AD cases showed elevated vascular and intracellular apoD immunostaining which localized primarily to cells clustered within plaques and around large blood vessels. ApoD-immunoreactive cells within plaques morphologically matched MHC-II- and CD-68-immunoreactive microglia, and did not contain the astrocytic marker GFAP, which labeled a subset of apoD-immunoreactive cells surrounding plaques. These data suggest that neuropil deposits of apoD localize only to a subset of Aβ plaques, which contain compact aggregates of fibrillar Aβ. Elevated apoD in AD brain may influence Aβ aggregation, or facilitate phagocytosis and transport of Aβ fibrils from plaques to cerebral vasculature.

Keywords: Alzheimer's disease; Amyloidosis; Apolipoprotein; Astrocyte; Microglia; Neuritic plaque; Neurodegeneration; Temporal cortex

Introduction

Pathogenesis of senile plaques in Alzheimer's disease (AD) may involve interactions between amyloid-beta (Aβ) peptide and apolipoproteins. Inheritance of allelic variation *ε4* of the apolipoprotein E (apoE) gene increases the extent of Aβ plaque formation (Rebeck et al., 1993; Schmechel et al., 1993) and risk of developing late-onset AD (Hardy, 1996; Kamboh, 1995; Strittmatter et al., 1993a). Apolipoprotein levels are elevated in AD brain (apoE, apoD, apoJ; Belloir et al., 2001; Kalman et al., 2000; Lidstrom et al., 1998; Terrisse et al., 1998; Yamada et al., 1995; Yamagata et al., 2001) where they localize to neuropil plaques co-labeled with either Aβ peptide antibodies (apoE, apoA-1, apoB, apoJ; Calero et al., 2000; Dickson et al., 1997; Gearing et al., 1995; Harr et al., 1996; Kida et al., 1994; Mufson et al., 1994; Namba et al., 1992; Sheng et al., 1996; Wisniewski and Frangione, 1992), or markers of the β-pleated sheet protein conformation (apoE, apoD; Mufson et al., 1994; Navarro et al., 2003). The binding affinity of apoE for Aβ, its ability to induce Aβ fibril formation (Strittmatter et al., 1993b; Vickers et al., 2000; Wisniewski et al., 1993, 1994), and its distribution pattern in Aβ-containing plaques (Dickson et al., 1997) may reflect its involvement in the fibrillization and deposition of Aβ into mature, dense-core neuritic plaques, or alternatively it may act to help clearance of Aβ from the brain (Dickson, 1997; Holtzman, 2001; Manelli et al., 2004). ApoD may also play a role in the development of Aβ-related pathology (Thomas et al., 2001); considering the general physiological role of this apolipoprotein in maintenance and repair in central and peripheral nervous systems (reviewed in Rassart et al., 2000), it may function to prevent Aβ fibril formation (Navarro et al., 2003) or, similar to apoJ, to facilitate clearance of Aβ from the neuropil (Calero et al., 2000; Rosenberg et al., 1993; Zlokovic et al., 1994). Despite possible functional similarities between apoD and apoE, these proteins showed different localization and changes in AD brain (Navarro et al., 2003; Terrisse et al., 1998; Thomas et al., 2003), and the

☆ Support: NIA AG13672 and NIA AG05133.
* Corresponding author. Department of Human Genetics, Graduate School of Public Health, University of Pittsburgh, Pittsburgh, PA 15261, USA. Fax: +1 412 383 7844.
E-mail address: ilyas.kamboh@mail.hgen.pitt.edu (M.I. Kamboh).
[1] Both authors contributed equally to this work.
Available online on ScienceDirect (www.sciencedirect.com).

0969-9961/$ - see front matter © 2005 Elsevier Inc. All rights reserved.
doi:10.1016/j.nbd.2005.04.012

relationship between apoD protein and AD pathology has been controversial. Because apoD plaques were detected in AD tissue (del Valle et al., 2003; Navarro et al., 1998, 2003), they were postulated to co-localize with Aβ (Navarro et al., 2003). However, Congo red histochemistry, not Aβ-specific antibodies, was employed by Navarro and colleagues, and thus the pattern of apoD protein in various forms of Aβ plaques is currently unknown. In the present study, we sought to determine the relationship between apoD and Aβ in plaques directly, by assessing the pattern and degree of co-localization of the two peptides using dual immunofluorescence and dual chromogen immunohistochemistry (IHC) with apoD and Aβ antibodies, in addition to histostaining of the β-pleated sheet protein conformation. We hypothesized that apoD is associated preferentially with compact plaques that contain dense aggregates of Aβ in the fibrillar β-pleated sheet conformation.

Methods

Paraformaldehyde-fixed middle temporal cortex tissue for IHC was obtained postmortem from 36 subjects with clinically diagnosed and autopsy-confirmed AD and 12 non-demented control individuals; the two groups were matched for age and postmortem interval (Table 2). Fresh-frozen middle temporal cortex tissue for Western blotting (WB) was available from 20 subjects in this cohort (15 AD patients, aged 59–85 years, and 5 controls, aged 62–75 years). AD patients were all diagnosed and followed in the University of Pittsburgh Alzheimer's Disease Research Center (ADRC), while controls were cognitively and neuropathologically normal individuals who were drawn from autopsy cases at the University of Pittsburgh Medical Center. Clinical diagnosis, tissue acquisition, and processing were performed as described previously (Ikonomovic et al., 2004; Lopez et al., 2000).

Antibody preabsorption and WB analysis

For preabsorption testing, human anti-apoD antisera (see Table 1 for details of antibodies used in this study) were incubated with excess (1:100) apoD protein (Signet Laboratories Inc., Dedham, MA) for 1 h at 4°C, followed by the IHC procedure as outlined below. WB analysis was performed by electrophoretically separating 10 μg of apoD protein and Aβ peptide (Sigma, St. Louis, MO) on a 10% Bis–Tris–HCl gel for 1 h at 21°C and transferring to a nitrocellulose membrane. After incubating in blocking solution (Tris buffered, pH 7.2, 5% nonfat dry milk and 1% Tween-20) at 4°C, blots were divided in half, and incubated overnight at 4°C with either anti-apoD or anti-Aβ (6E10) antisera dissolved in Tris-buffered saline (pH 7.2) with 1% Tween-20. Bound antisera were detected by incubating with horseradish peroxidase-conjugated goat anti-mouse IgG secondary antisera (1:2500; Vector Labs, Burlingame, CA) for 1 h at 21°C. Proteins were visualized by chemiluminescence detection system (Pierce, Rockford, IL).

IHC and ThioS/X-34 histostaining

IHC procedures were performed as previously described (Ikonomovic et al., 2004) on six tissue sections per case. For apoD immunodetection, free-floating tissue sections were incubated overnight with the apoD antibody. Sections were treated with an affinity-purified biotinylated secondary antibody generated against mouse IgG (1:250, American Qualex, San Clemente, CA), followed by the avidin–biotin peroxidase complex (1:200, Vector Labs, Burlingame, CA). The antigen–antibody reaction was visualized using hydrogen peroxide reaction in imidazole acetate buffer with diaminobenzidine (DAB) and nickel ammonium sulfate. Tissue sections from AD and control cases were processed simultaneously. For all subjects, sections near-adjacent to those processed for apoD were immunostained with Aβ antibody 6E10, to compare overall distribution patterns of Aβ and apoD plaques. IHC with 6E10 required pre-treatment of tissue sections with 80% formic acid (FA) for 2 min. For each case, three randomly selected apoD-immunolabeled tissue sections were counterstained with ThioS and X-34 (Table 1) to detect Aβ protein in the fibrillar β-pleated sheet conformation. At least one additional section was stained with NeuN to determine the cytoarchitectural boundaries of cortical lamina. Two tissue sections immediately adjacent to apoD-immunostained sections were immunostained using monoclonal antibodies generated against the major histo-compatibilty complex (MHC-II) and cluster differentiation 68 (CD-68), antigens commonly found on cells of macrophage/monocyte lineage. Images were captured and archived using Optimas 5.1 image analysis software (Optimas, Seattle, WA). Image manipulations were limited to cropping, resizing, and optimizing the brightness/contrast using Adobe Photoshop 5.0 software (Adobe Systems Incorporated, San Jose, CA).

Table 1
Summary of histofluorescent markers and antisera used for histological, immunohistochemical, and Western blot analyses

Histofluorescent cmpd	Affinity	Concentration	Source (reference)
Thioflavin S	β-pleated sheet	0.05%	Sigma (Guntern et al., 1992)
X-34	β-pleated sheet	100 nM	Dr. W.E. Klunk (Styren et al., 2000)
Antisera (host)	**Immunogen/clone**	**Dilution (application)**	**Source (reference)**
apoD (mouse)	8CD6[a]	1:1000 (IHC); 1:1000 (WB)	Calbiochem (current study)
6E10 or b6E10 (mouse)	$A\beta_{1-17}$	1:2000 (IHC) or 1:1000 (WB)	Signet (Kim et al., 1990)
Aβ40/42 (rabbit)	$A\beta_{1-40/42}$	1:100 (IHC)	Chemicon (Ghoshal et al., 2001)
NeuN (mouse)	A60[a]	1:750 (IHC)	Chemicon (Mullen et al., 1992)
GFAP (rabbit)	human GFAP	1:1000 (IHC)	Sigma (Götz et al., 2001)
MHC-II (mouse)	LN3[a]	1:2000 (IHC)	NeoMarkers (Perlmutter et al., 1992)
CD-68 (mouse)	KP1[a]	1:50 (IHC)	Zymed (Pulford et al., 1989)

b = Biotinylated.
[a] Clone.

Dual IHC

At least three sections per case were double-immunolabeled for simultaneous detection of apoD with Aβ plaques or GFAP-containing astrocytes. For immunofluorescence double-labeling, tissue sections were processed first with the apoD antibody and a fluorescein isothiocyanate (FITC)-conjugated secondary anti-mouse IgG antibody (Jackson Immuno Research Labs, West Grove, PA), and then double-labeled with either a rabbit polyclonal antibody against human Aβ (anti-$A\beta_{40/42}$) or a rabbit polyclonal anti-GFAP antibody, and a rhodamine-conjugated anti-rabbit IgG secondary antibody (Jackson). For dual chromogen IHC at the light microscopy level, sections were processed first for apoD using an alkaline phosphatase-conjugated anti-mouse IgG secondary antibody and the Vector blue substrate (Vector), and then double-labeled with a biotinylated anti-Aβ antibody (biotinylated 6E10, with 80% FA and mouse serum pre-treatment) or a polyclonal anti-GFAP antibody. The biotinylated anti-Aβ antibody was visualized directly using the avidin–biotin peroxidase procedure with DAB. The anti-GFAP antibody was first bound to a biotinylated anti-rabbit IgG secondary antibody and then visualized with DAB as described above. Levamisole was used to block endogenous alkaline phosphatase activity. To control for non-specific immunostaining in double-labeling procedures, either primary or secondary antibodies were omitted; alternatively, tissue sections were incubated with a non-specific secondary IgG and then processed as described. These negative controls always resulted in absence of immunostaining. Immunofluorescence was visualized using filters detecting emission peaks at 518 nm (FITC) and 580 nm (rhodamine). Fluorescent images are presented individually or as a combination using an overlay option of Adobe Photoshop 5.0 software.

Quantitation of apoD and Aβ plaques

Semi-quantitative evaluations of apoD and Aβ plaque frequencies in the middle temporal cortex were performed by a neuropathologist (RLH) as previously described (Ikonomovic et al., 2004).

Quantitative estimation of plaque load and percent co-localization was performed using the point counting method (Bussiere et al., 2002).

Terminology

We used the term "plaques" when referring to extracellular deposits of immunoreactive material in the neuropil, immunostained with antisera recognizing the proteins of interest (i.e., apoD or Aβ). When describing Aβ plaques, we use the term "diffuse plaques" to refer to amorphous or poorly circumscribed neuropil deposits of Aβ with no associated ThioS or X-34 staining, and the term "compact plaques" to refer to Aβ deposits that were more prominently immunostained, circular in the plane of section, with dense aggregates (see Dickson, 1997) of Aβ in the fibrillar (β-pleated sheet) form stained with ThioS or X-34 fluorescence. The same terms were avoided when describing apoD plaques, because they were morphologically distinct from Aβ plaques, involving not only extracellular but also substantial intracellular apoD immunostaining. The main prerequisite for apoD-immunoreactive "plaque" was the presence of a detectable neuropil immunostaining in the form of a clearly defined deposit (see Results), regardless of the extent of involvement of apoD-immunoreactive cells.

Prominent cellular constituents of compact Aβ plaques in AD temporal cortex are microglia and astrocytes (Itagaki et al., 1989). We immunohistochemically distinguished between apoD-immunoreactive astrocytes and microglia by double-labeling IHC with apoD and a polyclonal anti-GFAP antibody (an astrocytic marker). In addition, MHC-II and CD-68 antibodies were applied in immediately adjacent tissue sections to define the morphological characteristics and localization pattern of microglia. The apoD-immunoreactive/GFAP-negative glia were referred to as "microglia" since they lacked GFAP immunoreactivity of astrocytes, and they matched the specific pattern of MHC-II and CD-68 immunoreactive cells in the same cases, with morphological appearance and characteristic clustering typical of microglia within compact plaques as described previously (D'Andrea et al., 2004; Itagaki et al., 1989; Perlmutter et al., 1992).

Results

ApoD antibody characterization

We used IHC and WB analyses to examine (1) the specificity of our apoD antibody for synthetic human apoD

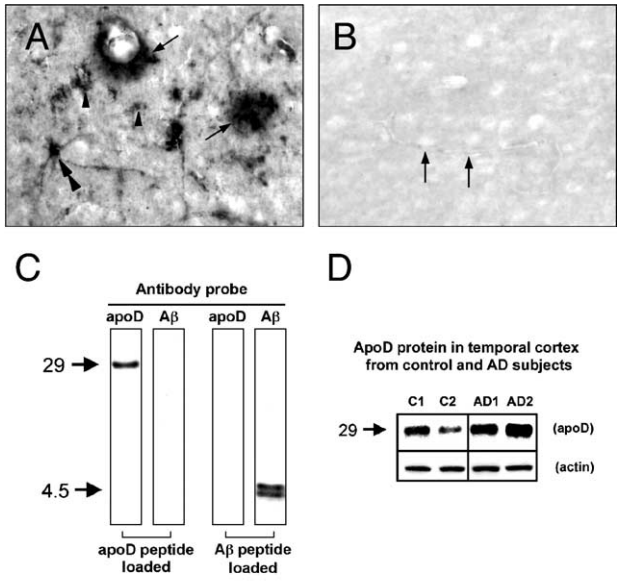

Fig. 1. Immunohistochemical and Western blot characterization of the apoD antibody used in this investigation. (A) AD temporal cortex with a typical pattern of apoD immunoreactivity in glia (arrowheads), isolated neurons (double arrowhead), and perivascular or neuropil plaque deposits (arrows). (B) An adjacent tissue section incubated with apoD antibody preabsorbed with apoD protein shows no immunostaining (an unstained blood vessel is indicated by arrows). (C) Western blot analysis demonstrates that apoD and Aβ antibodies, used in the co-localization experiments in this study, specifically recognize appropriate antigens and do not cross react. (D) Western blot analysis of temporal cortex gray matter from two representative non-demented controls (C1–2) and two AD cases shows considerable variability in apoD protein levels in controls and an increase in AD, further confirming the specificity of the apoD antibody. Scale bar = 50 μm.

protein and apoD protein in human brain tissue, and (2) potential cross reactivity of the apoD and Aβ antibodies used in this study with Aβ or apoD protein, respectively. AD temporal cortex tissue sections contained apoD-immunoreactive cells, blood vessels, and neuropil plaques. Preincubation of the apoD antisera with purified synthetic apoD protein prevented cell, vessel, and plaque immunostaining (Figs. 1A, B). Omission of the primary antisera from the IHC protocol, or incubation with an unrelated IgG, resulted in no detectable immunostaining (not shown), confirming the specificity of the secondary antibody reaction. WB analysis using purified apoD protein and Aβ peptide showed no cross reactivity for Aβ and apoD antibodies, as each antibody formed an immune complex exclusively with its corresponding protein (Figs. 1C, D). WB analysis of temporal cortex tissue homogenates from AD and control subjects showed that apoD protein levels are significantly increased in AD patients (Fig. 1D; Table 2), confirming previous reports of apoD protein upregulation in AD (Belloir et al., 2001; Glockner and Ohm, 2003; Terrisse et al., 1998; Thomas et al., 2003).

ApoD and Aβ in temporal cortex from control and AD subjects—single-immunolabeling studies

We next compared apoD immunostaining in a large cohort of AD and control patients, to determine the localization of elevated apoD protein that we observed by WB analysis. In our aged controls, apoD immunoreactivity was detected in glia and blood vessels (Fig. 2), and Aβ- and apoD-immunoreactive plaques were not observed (Table 2). In the gray matter, apoD immunoreactivity was observed in glial cell processes, predominantly along the more superficial cortical layers. In the white matter, oligodendroglial cells were apoD positive (not shown). AD temporal cortex contained increased immunostaining intensity and numbers of apoD-immunoreactive glial cells and blood vessels in the gray matter (Fig. 2), and oligodendroglia in the white matter (Fig. 3B). ApoD immunostaining in small-caliber blood vessels (5–20 μm) was patchy and confined to the vascular walls. Large-diameter blood vessels (>20 μm) were more intensely immunostained, with apoD observed throughout the vascular wall (see Fig. 5F), most prominently in the external layers, and in adjacent clusters of robustly apoD-immunoreactive putative perivascular microglia (Fig. 2D). Aβ-immunoreactive and apoD-immunoreactive plaques were detected in all AD

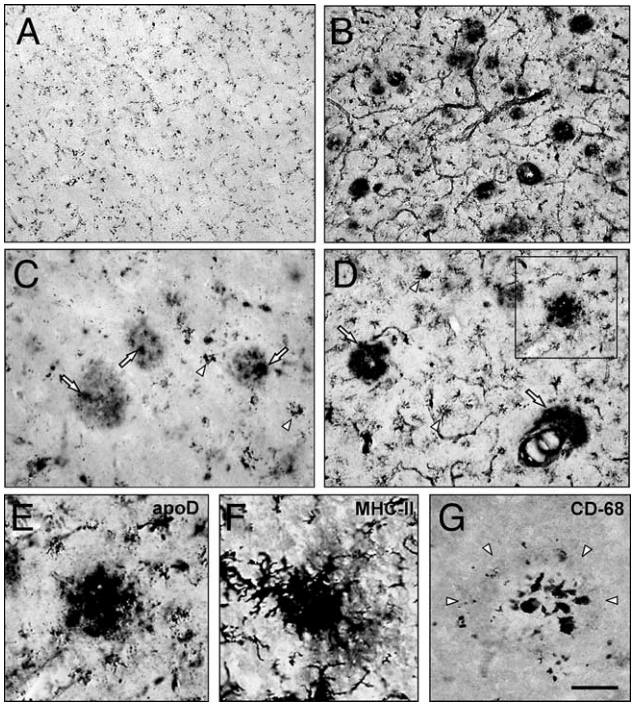

Fig. 2. ApoD immunoreactivity in the temporal cortex from non-demented control (A) and AD subjects (B–G). (A) In control subject, apoD immunoreactivity is localized to glial cells and blood vessels. (B) AD temporal cortex shows more intense apoD labeling of glial and vascular elements, as well as numerous apoD-immunoreactive plaques and perivascular aggregates. (C,D) Higher-power photomicrographs of apoD plaque immunostaining reveal round-shaped apoD-immunoreactive cells inside apoD plaques. The density of these cells in plaques is proportional to the degree of the overall plaque and vascular apoD immunostaining. An AD case with minimal vascular immunostaining shows apoD plaques with lightly increased neuropil immunostaining and a few plaque-associated (arrows) or free-standing (arrowheads) glia (C). An AD case with more prominent vascular immunostaining displays darker apoD plaques with numerous, intensely apoD-immunoreactive glia clustered within plaques or around large blood vessel lumen (arrows), while many apoD-immunoreactive glia are seen free-standing (arrowheads) in the neuropil (D). (E–G) Three adjacent sections from temporal cortex of an AD case, immunostained with apoD (E represents the area boxed in D) or microglia markers, illustrate the similarity between apoD- and MHC-II- or CD-68-immunoreactive cells clustering inside plaques (arrow heads in G). Scale bar = 100 μm (A,B), 50 μm (C,D), and 25 μm (E–G).

Table 2
Demographic data, results of plaque analyses, and apoD protein measurements in temporal cortex from AD subjects and non-demented controls

	AD (n = 36)	Controls (n = 12)
Age (years)		
Mean ± SD (range)	78 ± 8.8 (59–99)	63 ± 10.1 (49–75)
Gender		
Male/Female	17/19	9/3
PMI (h)		
Mean ± SD (range)	6.4 ± 4.2 (2–21)	10.5 ± 4.9 (3.5–18)
Plaque frequency scores		
apoD plaque score[a] (n)	0 (0); 1 (3); 2 (19); 3 (14)	0 (12); 1 (0); 2 (0); 3 (0)
Aβ plaque score[a] (n)	0 (0); 1 (0); 2 (3); 3 (33)	0 (12); 1 (0); 2 (0); 3 (0)
% Plaque co-localization		
Aβ with apoD	63 ± 9.3	N/A
apoD with Aβ	100	N/A
ThioS/X-34 with apoD	100	N/A
apoD with ThioS/X-34	100	N/A
Plaque score comparison		
apoD < Aβ	n = 21	N/A
apoD = Aβ	n = 15	N/A
apoD > Aβ	n = 0	N/A
ApoD protein levels (WB R.O.D.)	413.87 ± 88.9[b] (n = 15)	100 ± 15.5 (n = 5)

n = Number of cases; PMI = postmortem interval; WB = Western blot; R.O.D. = relative optical density.

[a] Plaque pathology scored as absent (0), mild (1), moderate (2), or severe (3).

[b] $P_{2\text{-tailed}} < 0.01$ (R.O.D. normalized to control levels).

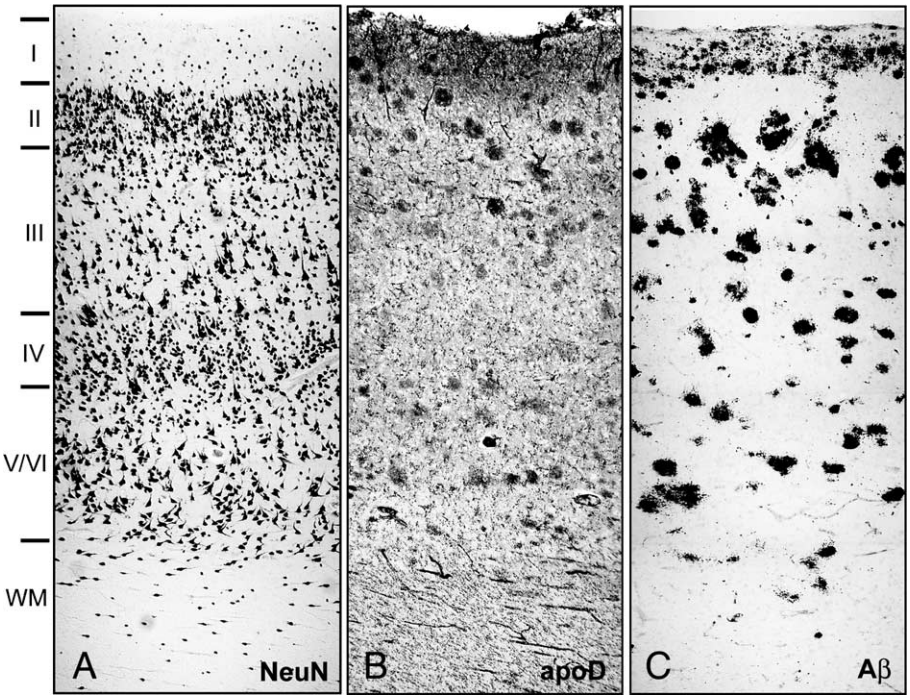

Fig. 3. Photomicrographic composites on adjacent sections of AD temporal cortex immunostained for the neuronal antigen NeuN (A), which delineates cortical layers I–VI, apoD (B), and 6E10 (C) antibodies. There is a similar overall distribution pattern of apoD and Aβ plaques across cortical layers. In layers III–IV, apoD plaques show lighter immunoreactivity compared to Aβ plaques. WM = white matter.

patients, in all cortical layers. Aβ plaques were more abundant than apoD plaques (Table 2), and their immunostaining intensity was consistent across cortical layers (Fig. 3). They were morphologically more variable than apoD plaques, forming either diffuse (irregular shape) or compact (circular shape, <200 μm diameter) neuropil deposits. ApoD plaques were circular in the plane of section, and varied in size (approximately. 50–200 μm diameter) and immunostaining intensity. Lightly immunostained apoD plaques were observed in layers III–IV, and more robustly immunostained plaques in superficial and deep cortical layers (Fig. 3). The overall intensity of apoD plaque immunostaining correlated directly with numbers of robustly apoD-immunoreactive cells, which were regularly observed within apoD plaques (Fig. 2), and with the degree of apoD immunoreactivity in the adjacent cerebral vasculature. ApoD plaques that contained fewer apoD-immunoreactive cells showed lighter immunostaining and were typically associated with light apoD immunoreactivity in blood vessels (Fig. 2C). In contrast, areas with intensely immunostained apoD plaques, densely packed with robustly apoD-immunoreactive cells, also contained more intensely apoD-immunostained blood vessels (Figs. 2B, D). Dense clustering of apoD-immunoreactive cells inside apoD plaques resulted in a "cored" appearance of plaques. However, such apoD plaques were distinct from cored Aβ plaques because their "core" region consisted of clusters of apoD-immunoreactive cells, rather than densely aggregated extracellular protein as seen in Aβ plaques. ApoD-immunoreactive cells within plaques matched the morphology and distribution pattern of MHC-II- and CD-68-immunoreactive microglia observed in similar plaque-like clusters in immediately adjacent tissue sections (Fig. 2).

Counterstaining of apoD-immunostained sections with ThioS and X-34, fluorescent markers of the β-pleated sheet protein conformation, revealed that all apoD-immunoreactive plaques were labeled with ThioS/X-34 and vice versa (Table 2, Fig. 4). The intensity of ThioS/X-34 fluorescence varied proportionally with the density of apoD-immunoreactive cells inside plaques, but the cells themselves were not fluorescent. Small-caliber blood vessels immunoreactive for apoD were ThioS/X-34 negative (Fig. 4). Large vessels with substantial amyloid angiopathy and apoD immunoreactivity were ThioS/X-34 positive (not shown).

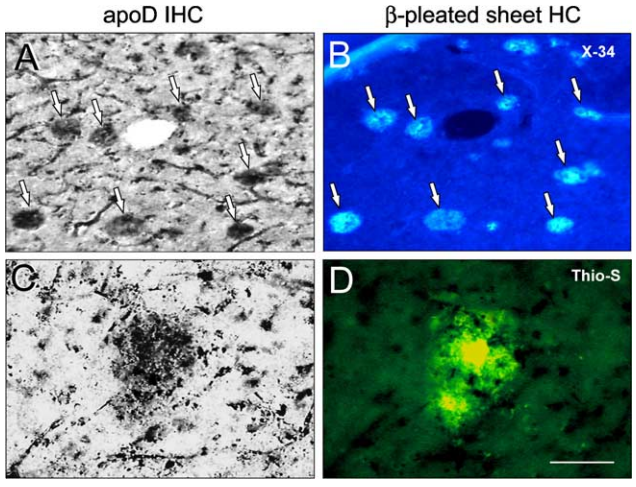

Fig. 4. Paired light/fluorescent microscopic images of dual apoD immunohistochemistry (IHC)/fluorescent histochemistry (HC) in the temporal cortex of an AD subject. (A–B) All apoD deposits (arrows) are labeled with X-34, while numerous apoD-immunoreactive capillaries are X-34 negative. (C,D) Higher-magnification images of a large plaque associated with apoD-immunoreactive glia that also contains ThioS fluorescence. Scale bar = 200 μm (A,B), 100 μm (C,D).

ApoD and Aβ in AD temporal cortex—double-immunolabeling studies

All apoD-immunoreactive plaques also contained Aβ, while only 63% of Aβ-immunoreactive plaques contained apoD (Table 2). Similar patterns of apoD/Aβ double-labeling were observed using fluorescent IHC with apoD and the C-terminus antibody $A\beta_{40/42}$ (Figs. 5A, B), and dual chromogen IHC with apoD and the $A\beta_{1-17}$ antibody against the amino terminus of the Aβ peptide (Fig. 5C). In dual-labeled plaques, apoD immunoreactivity was robust inside cells and less prominent in the neuropil, and Aβ immunoreactivity was extracellular. Dual-labeling for apoD and GFAP was performed to better characterize intracellular apoD immunostaining in and around apoD plaques (Figs. 5D, E). Punctate apoD immunoreactivity was observed in processes of GFAP-immunoreactive astrocytes throughout the temporal cortex, and more prominently in cell bodies and processes of large ramified astrocytes at the periphery of plaques in the plane of section. ApoD-immunoreactive cells inside plaques (putative microglia) were not GFAP-immunoreactive.

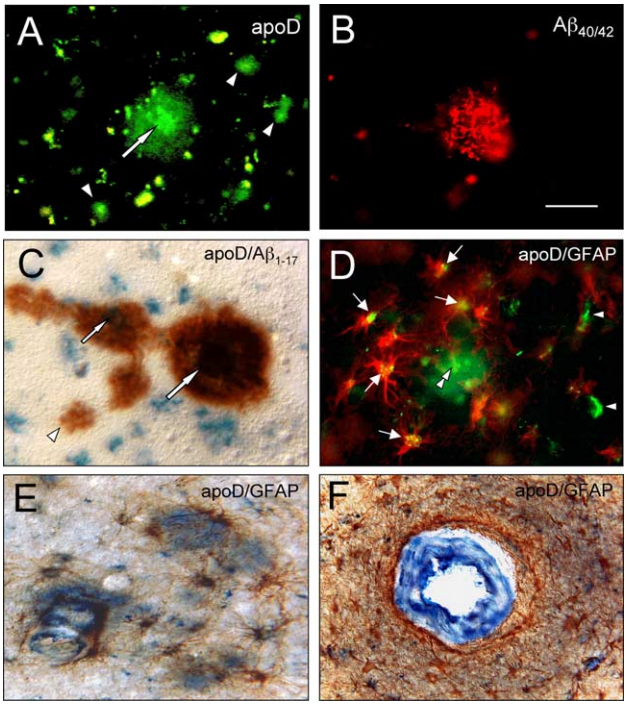

Fig. 5. Co-distribution of apoD with Aβ (A–C) or GFAP (D–F) in the temporal cortex of AD patients. (A,B) Paired fluorescent microscopic images of dual immunofluorescence for apoD (green) and the carboxy terminus of Aβ (red) show that the two peptides are localized to the same plaque. ApoD-immunoreactive cell elements are clustered in the plaque center (arrow) or scattered in the neuropil (arrowheads), while $A\beta_{40/42}$ staining is distributed throughout the plaque. (C) Dual chromogen immunohistochemistry for apoD (blue) and the amino terminus of Aβ (brown) shows co-distribution of the peptides in large compact plaques, with apoD concentrated in the center (arrows). Smaller diffuse Aβ plaque is free of apoD (arrowhead). (D,E) Fluorescence and bright field microscopy of double immunohistochemistry for apoD and GFAP (D: apoD-green/GFAP-red; E: apoD-blue/GFAP-brown) illustrate that GFAP-immunoreactive astrocytes are restricted to the periphery of apoD plaques, while GFAP-negative apoD-immunoreactive cells are mainly inside plaques (double arrowhead in D). GFAP-immunoreactive astrocytes contain granular apoD material (arrows in D), while some apoD+/GFAP− cells are observed in the neuropil (arrowheads in D). (F) Bright field of dual-label immunohistochemistry for apoD (blue) and GFAP (brown) shows apoD immunostaining in the wall of a large-caliber blood vessel, surrounded by GFAP-immunoreactive astrocytes. Scale bar = 75 μm (A–E), 100 μm (F).

Discussion

This report describes the relationship of intra- and extracellular apoD immunoreactivity with Aβ plaques in the temporal cortex of AD patients. The robust apoD immunostaining in plaques likely contributes to the high levels of apoD protein in AD brains as confirmed biochemically in this, and other (Belloir et al., 2001; Glockner and Ohm, 2003; Terrisse et al., 1998; Thomas et al., 2003) studies, and suggests a role for apoD in Aβ-related pathology of AD. Our immunohistochemical data demonstrate that apoD localizes primarily to compact fibrillar Aβ plaques, and is rare if not absent in diffuse Aβ plaques. Although the sequence of apoD and Aβ deposition in plaques is not known, these data suggest that, like apoE (Holtzman, 2001), apoD may be involved in the conversion of Aβ into aggregated fibrils that contribute to development of neuritic abnormalities in AD (reviewed in Yankner, 1996).

The current study confirmed and extended previous descriptions of apoD immunostaining in human brain (Navarro et al., 1998). Localization of apoD to plaques in AD brains was reported in some (del Valle et al., 2003; Navarro et al., 1998, 2003), but not all studies (Belloir et al., 2001; Kalman et al., 2000). This inconsistency could be due to differences in the apoD antibodies or tissue processing. Our data are in partial agreement with a recent study by Navarro and colleagues (Navarro et al., 2003), who reported apoD in some of the Congo-red-positive plaques in AD cortex. In contrast to the latter study, we found that apoD plaques always contained aggregated fibrillar (β-pleated sheet) material. This discrepancy could be due to different sensitivities of ThioS/X-34 and Congo red.

The present study found no detectable cross reactivity of the apoD antibody with Aβ peptide, or Aβ antibodies with apoD. One of the Aβ antibodies used in our study, 6E10, could potentially recognize secreted amyloid precursor protein (APP) in plaques; therefore, we confirmed our dual-labeling results using the $A\beta_{40/42}$ antibody, which is specific for the C-terminus of the Aβ peptide and cannot detect secreted forms of APP. With both of these antibodies, we demonstrated that apoD localizes to only a portion (63%) of Aβ plaques. The variability in the extent of apoD immunoreactivity in this study cannot be attributed to differences in tissue quality across subjects, as it was not observed in routine immunostaining for other plaque (e.g., Aβ) or cellular markers (e.g., GFAP, NeuN). It is also unlikely that the apoD immunostaining pattern was influenced by postmortem interval, because apoD peptide has been reported resistant to postmortem proteolytic degradation (Glockner and Ohm, 2003).

ApoD plaques contained numerous apoD-immunoreactive/GFAP-negative cells, which matched morphological features and distribution patterns of MHC-II- and CD-68-immunoreactive microglia in the present study and in the literature (D'Andrea et al., 2004; Perlmutter et al., 1992). While these observations suggest that apoD-immunoreactive/GFAP-negative cells within plaques are microglia, the precise identity of these cells cannot be determined absolutely in the absence of double-labeling IHC in single tissue sections. Similar to the proposed role for apoE (see LaDu et al., 2001, for review), apoD may be part of an inflammatory response

by reactive glial cells, which are likely responsible for the uptake and removal of fibrillar Aβ from the brain or, alternatively, for the conversion of Aβ to fibrils, as part of a dynamic process involving plaque evolution and resolution (D'Andrea et al., 2004; Hyman et al., 1993; Nagele et al., 2004; Rogers et al., 2002). ApoD is involved in binding and transport of small hydrophobic molecules including cholesterol (Patel et al., 1997), and increased levels during neurodegenerative and neuroregenerative responses support its role as an acute-phase protein, where it possibly engages in scavenging toxic hydrophobic compounds away from the site of injury (Seguin et al., 1995). As a carrier protein, apoD may facilitate Aβ removal from plaques by microglia which, subsequent to Aβ phagocytosis, migrate to blood vessels (Frautschy et al., 1992). The observations of robust apoD immunostaining in perivascular microglia and vascular walls in areas with amyloid angiopathy, and that the density of apoD-immunoreactive microglia in plaques was directly proportional to the degree of apoD immunoreactivity in cerebral vasculature, are in accord with this idea. These results are also in agreement with previous reports of apoD-immunoreactive perivascular cells (Hu et al., 2001; Kalman et al., 2000; Navarro et al., 1998, 2003). The presence of non-cellular (neuropil) apoD immunostaining in plaques, and its co-distribution with Aβ, may reflect protein–protein interactions during Aβ sequestration by plaque-associated macrophages.

ApoD immunostaining of neurons was scarce in the present study, and very few apoD-immunoreactive cells resembled neurofibrillary tangles (NFT). This is consistent with the previous immunohistochemical study by Belloir et al. (2001), who found that less than 1% of hippocampal neurons was double-labeled with apoD and tau. Glockner and Ohm (2003) reported that increased cortical apoD levels were influenced by more severe NFT pathology as defined by Braak and Braak (1991), and that hippocampal apoD levels were also higher in cases with more advanced plaque pathology (although the latter did not reach statistical significance). It is difficult to draw comparisons between the present immunohistochemical study and biochemical studies comparing regional measurements of apoD protein levels with a general measure of NFT/plaque pathology in the brain, especially given the diverse cellular and neuropil localization potentially contributing to elevated apoD in AD. Different apoD levels between high versus low Braak groups, observed by Glockner and Ohm (2003), could be interpreted as disease-specific, because all of the cases with neocortical NFT pathology (Braak V/VI stage) had AD, while those subjects with NFTs absent or confined to the transentorhinal area (Braak 0–I/II) were non-demented controls. The role of apoD in the complex milieu of neuropathological changes in AD brains remains to be investigated.

In summary, this study demonstrates that apoD is associated selectively with Aβ fibrils aggregated into compact AD plaques, and outlines a complex pattern of plaque-associated apoD-immunoreactive cells. The exact role of apoD in the complex interaction of microglial and astroglial cells with Aβ plaques remains to be determined. ApoD may function to facilitate aggregation of Aβ into the fibrillar β-pleated sheet conformation, or to sequester already aggregated fibrillar Aβ for removal from the brain parenchyma. ApoD could also function to transport molecules to the site of neuronal injury in AD brain, to facilitate remyelination and neuronal regeneration, which is consistent with increased apoD immunostaining of glial cells including oligodendroglia in the white matter (Hu et al., 2001; Navarro et al., 2004). Thus, the presence of apoD in compact Aβ plaques may in part reflect a reparative response to the development of dystrophic neurites, which are associated with more advanced (neuritic) Aβ plaque pathology.

Acknowledgments

We thank Dr. Geoffrey Murdoch for helpful discussions, and Mr. William R. Paljug for expert technical assistance.

References

Belloir, B., Kovari, E., Surini-Demiri, M., Savioz, A., 2001. Altered apolipoprotein D expression in the brain of patients with Alzheimer disease. J. Neurosci. Res. 64, 61–69.

Braak, H., Braak, E., 1991. Neuropathological staging of Alzheimer-related changes. Acta Neuropathol. 82, 239–259.

Bussiere, T., Friend, P.D., Sadeghi, N., Wicinski, B., Lin, G.I., Bouras, C., Giannakopoulos, P., Robakis, N.K., Morrison, J.H., Perl, D.P., Hof, P.R., 2002. Stereologic assessment of the total cortical volume occupied by amyloid deposits and its relationship with cognitive status in aging and Alzheimer's disease. Neuroscience 112, 75–91.

Calero, M., Rostagno, A., Matsubara, E., Zlokovic, B., Frangione, B., Ghiso, J., 2000. Apolipoprotein J (clusterin) and Alzheimer's disease. Microsc. Res. Tech. 50, 305–315.

D'Andrea, M.R., Cole, G.M., Ard, M.D., 2004. The microglial phagocytic role with specific plaque types in the Alzheimer's disease brain. Neurobiol. Aging 25, 675–683.

del Valle, E., Navarro, A., Astudillo, A., Tolivia, J., 2003. Apolipoprotein D expression in human brain reactive astrocytes. J. Histochem. Cytochem. 51, 1285–1290.

Dickson, D.W., 1997. The pathogenesis of senile plaques. J. Neuropathol. Exp. Neurol. 56, 321–339.

Dickson, T.C., Saunders, H.L., Vickers, J.C., 1997. Relationship between apolipoprotein E and the amyloid deposits and dystrophic neurites of Alzheimer's disease. Neuropathol. Appl. Neurobiol. 23, 483–491.

Frautschy, S.A., Cole, G.M., Baird, A., 1992. Phagocytosis and deposition of vascular beta-amyloid in rat brains injected with Alzheimer beta-amyloid. Am. J. Pathol. 140, 1389–1399.

Gearing, M., Schneider, J.A., Robbins, R.S., Hollister, R.D., Mori, H., Games, D., Hyman, B.T., Mirra, S.S., 1995. Regional variation in the distribution of apolipoprotein E and A beta in Alzheimer's disease. J. Neuropathol. Exp. Neurol. 54, 833–841.

Ghoshal, N., García-Sierra, F., Fu, Y., Beckett, L.A., Mufson, E.J., Kuret, J., Berry, R.W., Binder, L.I., 2001. Tau-66: evidence for a novel tau conformation in Alzheimer's disease. J. Neurochem. 77, 1372–1385.

Glockner, F., Ohm, T.G., 2003. Hippocampal apolipoprotein D level depends on Braak stage and APOE genotype. Neuroscience 122, 103–110.

Götz, J., Chen, F., Van Dorpe, J., Nitsch, R.M., 2001. Formation of neurofibrillary tangles in P301l tau transgenic mice induced by Abeta 42 fibrils. Science 293, 1491–1495.

Guntern, R., Bouras, C., Hof, P.R., Vallet, P.G., 1992. An improved thioflavine S method for staining neurofibrillary tangles and senile plaques in Alzheimer's disease. Experientia 48, 8–10.

Hardy, J., 1996. Molecular genetics of Alzheimer's disease. Acta Neurol. Scand. (Suppl.) 165, 13–17.

Harr, S.D., Uint, L., Hollister, R., Hyman, B.T., Mendez, A.J., 1996. Brain expression of apolipoproteins E, J, and A–I in Alzheimer's disease. J. Neurochem. 66, 2429–2435.

Holtzman, D.M., 2001. Role of apoe/Abeta interactions in the pathogenesis of Alzheimer's disease and cerebral amyloid angiopathy. J. Mol. Neurosci. 17, 147–155.

Hu, C.Y., Ong, W.Y., Sundaram, R.K., Chan, C., Patel, S.C., 2001.

Immunocytochemical localization of apolipoprotein D in oligodendrocyte precursor-like cells, perivascular cells, and pericytes in the human cerebral cortex. J. Neurocytol. 30, 209–218.

Hyman, B.T., Marzloff, K., Arriagada, P.V., 1993. The lack of accumulation of senile plaques or amyloid burden in Alzheimer's disease suggests a dynamic balance between amyloid deposition and resolution. J. Neuropathol. Exp. Neurol. 52, 594–600.

Ikonomovic, M.D., Uryu, K., Abrahamson, E.E., Ciallella, J.R., Trojanowski, J.Q., Lee, V.M.-Y., Clark, R.B.S., Marion, D.W., Wisniewski, S.R., DeKosky, S.T., 2004. Alzheimer's pathology in human temporal cortex surgically excised after severe brain injury. Exp. Neurol. 190, 192–203.

Itagaki, S., McGeer, P.L., Akiyama, H., Zhu, S., Selkoe, D., 1989. Relationship of microglia and astrocytes to amyloid deposits of Alzheimer disease. J. Neuroimmunol. 24, 173–182.

Kalman, J., McConathy, W., Araoz, C., Kasa, P., Lacko, A.G., 2000. Apolipoprotein D in the aging brain and in Alzheimer's dementia. Neurol. Res. 22, 330–336.

Kamboh, M.I., 1995. Apolipoprotein E polymorphism and susceptibility to Alzheimer's disease. Hum. Biol. 67, 195–215.

Kida, E., Golabek, A.A., Wisniewski, T., Wisniewski, K.E., 1994. Regional differences in apolipoprotein E immunoreactivity in diffuse plaques in Alzheimer's disease brain. Neurosci. Lett. 167, 73–76.

Kim, K.S., Wen, G.Y., Bancher, C., Chen, C.M.J., Sapienza, V.J., Hong, H., Wisniewski, H.M., 1990. Detection and quantitation of β-peptide with two monoclonal antibodies. Neurosci. Res. Commun. 7, 113–122.

LaDu, M.J., Shah, J.A., Reardon, C.A., Getz, G.S., Bu, G., Hu, J., Guo, L., Van Eldik, L.J., 2001. Apolipoprotein E and apolipoprotein E receptors modulate Abeta-induced glial neuroinflammatory responses. Neurochem. Int. 39, 427–434.

Lidstrom, A.M., Bogdanovic, N., Hesse, C., Volkman, I., Davidsson, P., Blennow, K., 1998. Clusterin (apolipoprotein J) protein levels are increased in hippocampus and in frontal cortex in Alzheimer's disease. Exp. Neurol. 154, 511–521.

Lopez, O.L., Becker, J.T., Klunk, W., Saxton, J., Hamilton, R.L., Kaufer, D.I., Sweet, R.A., Cidis Meltzer, C., Wisniewski, S., Kamboh, M.I., DeKosky, S.T., 2000. Research evaluation and diagnosis of probable Alzheimer's disease over the last two decades: I. Neurology 55, 1854–1862.

Manelli, A.M., Stine, W.B., Van Eldik, L.J., LaDu, M.J., 2004. ApoE and Abeta1-42 interactions: effects of isoform and conformation on structure and function. J. Mol. Neurosci. 23, 235–246.

Mufson, E.J., Benzing, W.C., Cole, G.M., Wang, H., Emerich, D.F., Sladek Jr., J.R., Morrison, J.H., Kordower, J.H., 1994. Apolipoprotein E-immunoreactivity in aged rhesus monkey cortex: colocalization with amyloid plaques. Neurobiol. Aging 15, 621–627.

Mullen, R.J., Buck, C.R., Smith, A.M., 1992. NeuN, a neuronal specific nuclear protein in vertebrates. Development 116, 201–211.

Nagele, R.G., Wegiel, J., Venkataraman, V., Imaki, H., Wang, K.C., Wegiel, J., 2004. Contribution of glial cells to the development of amyloid plaques in Alzheimer's disease. Neurobiol. Aging 25, 663–674.

Namba, Y., Tsuchiya, H., Ikeda, K., 1992. Apolipoprotein B immunoreactivity in senile plaque and vascular amyloid and neurofibrillary tangles in the brains of patients with Alzheimer's disease. Neurosci. Lett. 134, 264–266.

Navarro, A., Tolivia, J., Astudillo, A., del Valle, E., 1998. Pattern of apolipoprotein D immunoreactivity in human brain. Neurosci. Lett. 254, 17–20.

Navarro, A., Del Valle, E., Astudillo, A., Gonzalez del Rey, C., Tolivia, J., 2003. Immunohistochemical study of distribution of apolipoproteins E and D in human cerebral beta amyloid deposits. Exp. Neurol. 184, 697–704.

Navarro, A., del Valle, E., Tolivia, J., 2004. Differential expression of apolipoprotein D in human astroglial and oligodendroglial cells. J. Histochem. Cytochem. 52, 1031–1036.

Patel, R.C., Lange, D., McConathy, W.J., Patel, Y.C., Patel, S.C., 1997. Probing the structure of the ligand binding cavity of lipocalins by fluorescence spectroscopy. Protein Eng. 10, 621–625.

Perlmutter, L.S., Scott, S.A., Barron, E., Chui, H.C., 1992. MHC class II-positive microglia in human brain: association with Alzheimer lesions. J. Neurosci. Res. 33, 549–558.

Pulford, K.A., Rigney, E.M., Micklem, K.J., Jones, M., Stross, W.P., Gatter, K.C., Mason, D.Y., 1989. KP1: a new monoclonal antibody that detects a monocyte/macrophage associated antigen in routinely processed tissue sections. J. Clin. Pathol. 42, 414–421.

Rassart, E., Bedirian, A., Do Carmo, S., Guinard, O., Sirois, J., Terrisse, L., Milne, R., 2000. Apolipoprotein D. Biochim. Biophys. Acta 1482, 185–198.

Rebeck, G.W., Reiter, J.S., Strickland, D.K., Hyman, B.T., 1993. Apolipoprotein E in sporadic Alzheimer's disease: allelic variation and receptor interactions. Neuron 11, 575–580.

Rogers, J., Strohmeyer, R., Kovelowski, C.J., Li, R., 2002. Microglia and inflammatory mechanisms in the clearance of amyloid beta peptide. Glia 40, 260–269.

Rosenberg, M.E., Dvergsten, J., Correa-Rotter, R., 1993. Clusterin: an enigmatic protein recruited by diverse stimuli. J. Lab. Clin. Med. 121, 205–214.

Schmechel, D.E., Saunders, A.M., Strittmatter, W.J., Crain, B.J., Hulette, C.M., Joo, S.H., Pericak-Vance, M.A., Goldgaber, D., Roses, A.D., 1993. Increased amyloid beta-peptide deposition in cerebral cortex as a consequence of apolipoprotein E genotype in late-onset Alzheimer disease. Proc. Natl. Acad. Sci. U. S. A. 90, 9649–9653.

Seguin, D., Desforges, M., Rassart, E., 1995. Molecular characterization and differential mRNA tissue distribution of mouse apolipoprotein D. Brain Res. Mol. Brain Res. 30, 242–250.

Sheng, J.G., Mrak, R.E., Griffin, W.S., 1996. Apolipoprotein E distribution among different plaque types in Alzheimer's disease: implications for its role in plaque progression. Neuropathol. Appl. Neurobiol. 22, 334–341.

Strittmatter, W.J., Saunders, A.M., Schmechel, D., Pericak-Vance, M., Enghild, J., Salvesen, G.S., Roses, A.D., 1993a. Apolipoprotein E: high-avidity binding to beta-amyloid and increased frequency of type 4 allele in late-onset familial Alzheimer disease. Proc. Natl. Acad. Sci. U. S. A. 90, 1977–1981.

Strittmatter, W.J., Weisgraber, K.H., Huang, D.Y., Dong, L.M., Salvesen, G.S., Pericak-Vance, M., Schmechel, D., Saunders, A.M., Goldgaber, D., Roses, A.D., 1993b. Binding of human apolipoprotein E to synthetic amyloid beta peptide: isoform-specific effects and implications for late-onset Alzheimer disease. Proc. Natl. Acad. Sci. U. S. A. 90, 8098–8102.

Styren, S.D., Hamilton, R.L., Styren, G.C., Klunk, W.E., 2000. X-34, a fluorescent derivative of Congo red: a novel histochemical stain for Alzheimer's disease pathology. J. Histochem. Cytochem. 48, 1223–1232.

Terrisse, L., Poirier, J., Bertrand, P., Merched, A., Visvikis, S., Siest, G., Milne, R., Rassart, E., 1998. Increased levels of apolipoprotein D in cerebrospinal fluid and hippocampus of Alzheimer's patients. J. Neurochem. 71, 1643–1650.

Thomas, E.A., Sautkulis, L.N., Criado, J.R., Games, D., Sutcliffe, J.G., 2001. Apolipoprotein D mRNA expression is elevated in PDAPP transgenic mice. J. Neurochem. 79, 1059–1064.

Thomas, E.A., Laws, S.M., Sutcliffe, J.G., Harper, C., Dean, B., McClean, C., Masters, C., Lautenschlager, N., Gandy, S.E., Martins, R.N., 2003. Apolipoprotein D levels are elevated in prefrontal cortex of subjects with Alzheimer's disease: no relation to apolipoprotein E expression or genotype. Biol. Psychiatry 54, 136–141.

Vickers, J.C., Dickson, T.C., Adlard, P.A., Saunders, H.L., King, C.E., McCormack, G., 2000. The cause of neuronal degeneration in Alzheimer's disease. Prog. Neurobiol. 60, 139–165.

Wisniewski, T., Frangione, B., 1992. Apolipoprotein E: a pathological chaperone protein in patients with cerebral and systemic amyloid. Neurosci. Lett. 135, 235–238.

Wisniewski, T., Golabek, A., Matsubara, E., Ghiso, J., Frangione, B., 1993. Apolipoprotein E: binding to soluble Alzheimer's beta-amyloid. Biochem. Biophys. Res. Commun. 192, 359–365.

Wisniewski, T., Castano, E.M., Golabek, A., Vogel, T., Frangione, B., 1994. Acceleration of Alzheimer's fibril formation by apolipoprotein E in vitro. Am. J. Pathol. 145, 1030–1035.

Yamada, T., Kondo, A., Takamatsu, J., Tateishi, J., Goto, I., 1995. Apolipoprotein E mRNA in the brains of patients with Alzheimer's disease. J. Neurol. Sci. 129, 56–61.

Yamagata, K., Urakami, K., Ikeda, K., Ji, Y., Adachi, Y., Arai, H., Sasaki, H., Sato, K., Nakashima, K., 2001. High expression of apolipoprotein E mRNA in the brains with sporadic Alzheimer's disease. Dement. Geriatr. Cogn. Disord. 12, 57–62.

Yankner, B.A., 1996. Mechanisms of neuronal degeneration in Alzheimer's disease. Neuron 5, 921–932.

Zlokovic, B.V., Martel, C.L., Mackic, J.B., Matsubara, E., Wisniewski, T., McComb, J.G., Frangione, B., Ghiso, J., 1994. Brain uptake of circulating apolipoproteins J and E complexed to Alzheimer's amyloid beta. Biochem. Biophys. Res. Commun. 205, 1431–1437.